JOURNAL OF GEOPHYSICAL RESEARCH: SPACE PHYSICS, VOL. 118, 6511–6517, doi:10.1002/jgra.50586, 2013

Temporal and spatial precursors in ionospheric total electron content of the 16 October 1999 M_w7.1 Hector Mine earthquake

Y. C. Su,[1] J. Y. Liu,[1,2,3] S. P. Chen,[1] H. F. Tsai,[4] and M. Q. Chen[1,4]

Received 28 May 2013; revised 5 September 2013; accepted 20 September 2013; published 3 October 2013.

[1] In this paper, temporal and spatial analyses are employed to detect seismo-ionospheric precursors (SIPs) in the ionospheric total electron content (TEC) during the 16 October 1999 M_w7.1 Hector Mine earthquake. To discriminate anomalies caused by global effects, such as solar radiations, magnetic storms, etc., and local effects, such as earthquake, we cross-examine the GPS TECs and their gradients in the eastward and northward directions at epicenter/centers of the Hector Mine area and the other two reference areas at similar magnetic latitudes in Europe and Japan. Temporal variations of the northward TEC gradient suggest SIPs most likely appearing on days 6–5 before the earthquake. A global search by using the TEC of the global ionosphere map shows that the TEC increase and decrease anomalies continuously and specifically appear around the epicenter on day 5 before the earthquake.

Citation: Su, Y. C., J. Y. Liu, S. P. Chen, H. F. Tsai, and M. Q. Chen (2013), Temporal and spatial precursors in ionospheric total electron content of the 16 October 1999 M_w7.1 Hector Mine earthquake, *J. Geophys. Res. Space Physics*, *118*, 6511–6517, doi:10.1002/jgra.50586.

1. Introduction

[2] Anomalous phenomena in the ionosphere appearing before earthquakes have been reported [*Liu et al*., 2000, 2001, 2006, 2013a; *Hayakawa and Molchanov*, 2002; *Pulinets and Boyarchuk*, 2004; *Chen et al*., 2004]. *Liu et al*. [2001] first utilize the ionospheric total electron content (TEC), integrating the electron density from GPS satellites to ground-based receivers, to detect seismo-ionospheric precursors (SIPs) associated with large earthquakes, and find that TEC around the epicenters tends to anomalously decrease in the afternoon period a few days before the earthquakes in Taiwan. Based on *Liu et al*. [2001], many studies detecting SIPs by means of the GPS TEC have been carried out [e.g., *Liu et al*., 2004, 2006, 2009, 2010, 2011b; *Pulinets et al*., 2007; *Zhao et al*., 2008; *Kakinami et al*., 2010; *Jhuang et al*., 2010; *Le et al*., 2011, 2013; *Thomas et al*., 2012].

[3] The moment magnitude M_w7.1 Hector Mine, California earthquake occurred at 34.59°N, 116.27°W (60.5° geomagnetic inclination at 300 km high) on 16 October 1999 at 09:46 UT. *Pulinets et al*. [2007] proposed the regional variability index, which was the TEC difference between maximum and minimum values for every given moment derived from a network of ground-based GPS receivers around the epicenter, examining SIPs associated with the Hector Mine earthquake. They reported the growth of the regional variability 5 days before the seismic shock but did not find any increased variability for the periods of magnetic storms. However, *Thomas et al*. [2012] reproduced the regional variability index with the same GPS receiving network and cross-compared with that derived from a reference area of two GPS receivers in high latitudes and far away from the Hector Mine earthquake. They concluded that the anomalous signal identified by *Pulinets et al*. [2007] was just part of normal global-scale TEC variation and unrelated to the Hector Mine earthquake. Note that *Thomas et al*. [2012] adopted two GPS receivers in high latitudes to detect the global effect of magnetic storms. However, to conduct a sensible comparison, a reference GPS receiving network should be located in similar magnetic latitudes as the epicenter. Otherwise, a global comparison is required.

[4] The ionosphere can be easily disturbed by solar radiations, solar winds, magnetic storms, etc., which are termed global effects [cf. *Liu et al*., 2006; *Afraimovich and Astafyeva*, 2008]. In this study, to discriminate the global effects and local effects (such as earthquakes), a new technique using both temporal and spatial analyses is developed to examine the TEC derived from the epicenter and two reference areas in Europe and Japan, as well as extracted from the global ionosphere map (GIM from ftp://ftp.unibe.ch/aiub/CODE/) during 15 days before and after the earthquake. For the temporal analysis, the TEC and its gradients above the epicenter and those at the centers of the reference areas are investigated. Finally, the spatial analysis,

Additional supporting information may be found in the online version of this article.

[1]Institute of Space Science, National Central University, Jhongli, Taiwan.
[2]Center for Space and Remote Sensing Research, National Central University, Jhongli, Taiwan.
[3]National Space Organization, Hsinchu, Taiwan.
[4]GPS Science and Application Research Center, National Central University, Jhongli, Taiwan.

Corresponding author: J. Y. Liu, Institute of Space Science, National Central University, Jhongli 32001, Taiwan. (jyliu@jupiter.ss.ncu.edu.tw)

2169-9380/13/10.1002/jgra.50586

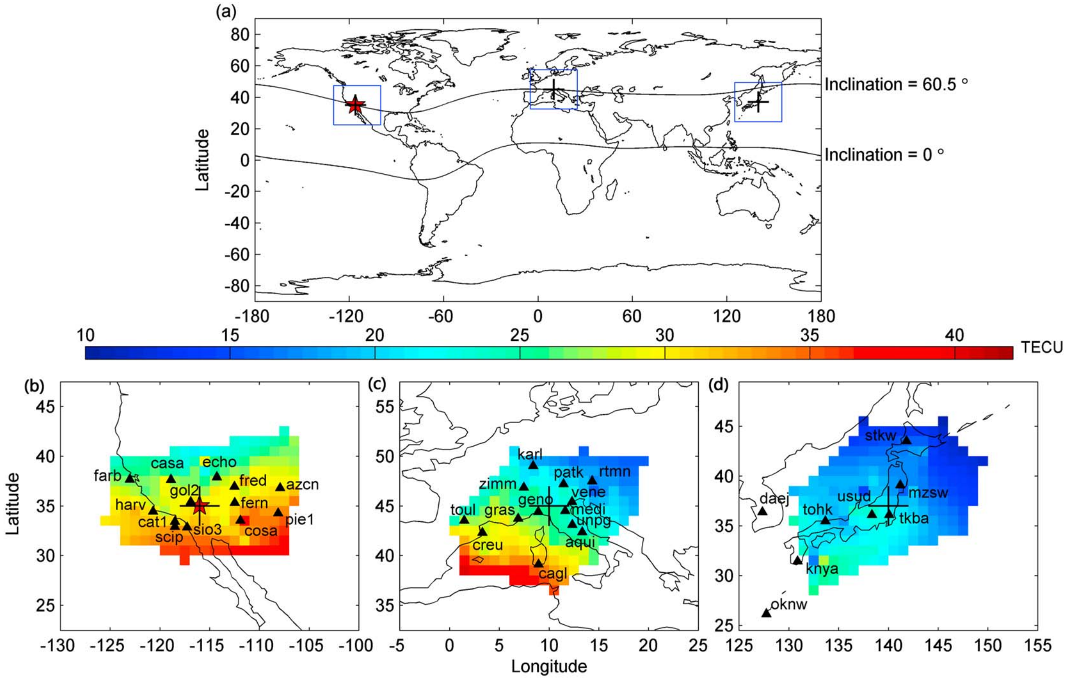

Figure 1. The Hector Mine area and two reference areas. (a) Global map. The red star and cross lines denote the epicenter and reference centers, respectively. Two black lines are the geomagnetic isoclinic lines of 60.5° and 0° at 300 km high. (b–d) GPS receiver locations in the Hector Mine and two references in Europe and Japan. Snapshots of 2-D GPS TEC with resolution of 1° × 1° in latitude and longitude can be derived every 30 s. The three snapshots were constructed at 17:00 UT on 16 October 1999. The length of the cross lines in longitude and latitude is 4°, which is used to compute the eastward and northward gradient.

SIPs of anomalous increases and decreases in the TEC continuously appearing in a sequence of GIMs, is introduced to find a possible location of the epicenter a few days before the earthquake.

2. Data Analysis

[5] Figure 1 illustrates that three ground-based GPS networks consist of 13 receivers in Hector Mine, 13 receivers in Europe, and 8 receivers in Japan. The 13 receivers in the Hector Mine area are identical to those listed in *Thomas et al*. [2012], and the epicenter is at geomagnetic inclination 60.5°. The centers of the Europe and Japan are at 45°N, 10°E (60.5° inclination) and 37°N, 140°E (50.5° inclination), respectively. Note that the three networks are at similar magnetic inclinations (latitudes) but separated by 110–130° in longitude. A TEC image/snapshot over each network can be constructed for every 30 s.

[6] We first present the space weather and geomagnetic condition as well as extract TECs over the centers of the three networks during October 1999. The $F_{10.7}$ index (10.7 cm solar radio flux) and the geomagnetic *Kp* and *Dst* indices indicate that the space weather and geomagnetic activity are relatively disturbed during 10–17 October 1999, 6 days before to 1 day after the earthquake (Figure 2a). The two geomagnetic indices reveal that multi-small storms occurred during the period, while an intense storm appeared during 21–24 October. Many increase anomalies of the TEC appear over the three centers within days 0–14 before the earthquake, on 2–16 October 1999 (Figure 2b), and especially prominent increases on 10–11 and 21–22 October 1999, as well as remarkable decreases on 22–23 October 1999.

[7] Based on the spirit of detecting SIPs by means of the spatial distribution proposed by *Pulinets et al*. [2007], we further compute the TEC gradient in the eastward and northward direction every 30 s. Figure 3a displays both increase and decrease anomalies in the eastward TEC gradients which sporadically appear at the three centers. Notice that a relative long duration of pronounced increase/decrease appears at the Hector Mine epicenter on the intense storm day, 22 October 1999. By contrast, Figure 3b illustrates that the northward TEC gradients at the three centers yield significant decrease anomalies during 10–11 October and the one over the Hector Mine epicenter obtains the most remarkable feature among the three on 10 October. It can be seen that the decrease anomalies over the three networks on 22 October triggered by the intense storm are weaker than those on 10–11 October.

[8] Although temporal variations of the TEC and associated gradients over the three networks have been examined, the remarkable decrease in the northward TEC gradient appearing over the epicenter, day 6 (10 October) before the Hector Mine earthquake, still might be coincident. To discriminate storm and earthquake effects, a global examination would be required. A dense network of GPS receivers is suitable to conduct TEC studies with a very fine space and rather high time resolution in its network area, while the GIM could be used to discriminate local and global effects. The GIM TEC maps with 2 h time resolution covering ±87.5°N latitude and ±180°E longitude ranges with spatial resolutions of 2.5° and 5°, respectively, are ideal to monitor

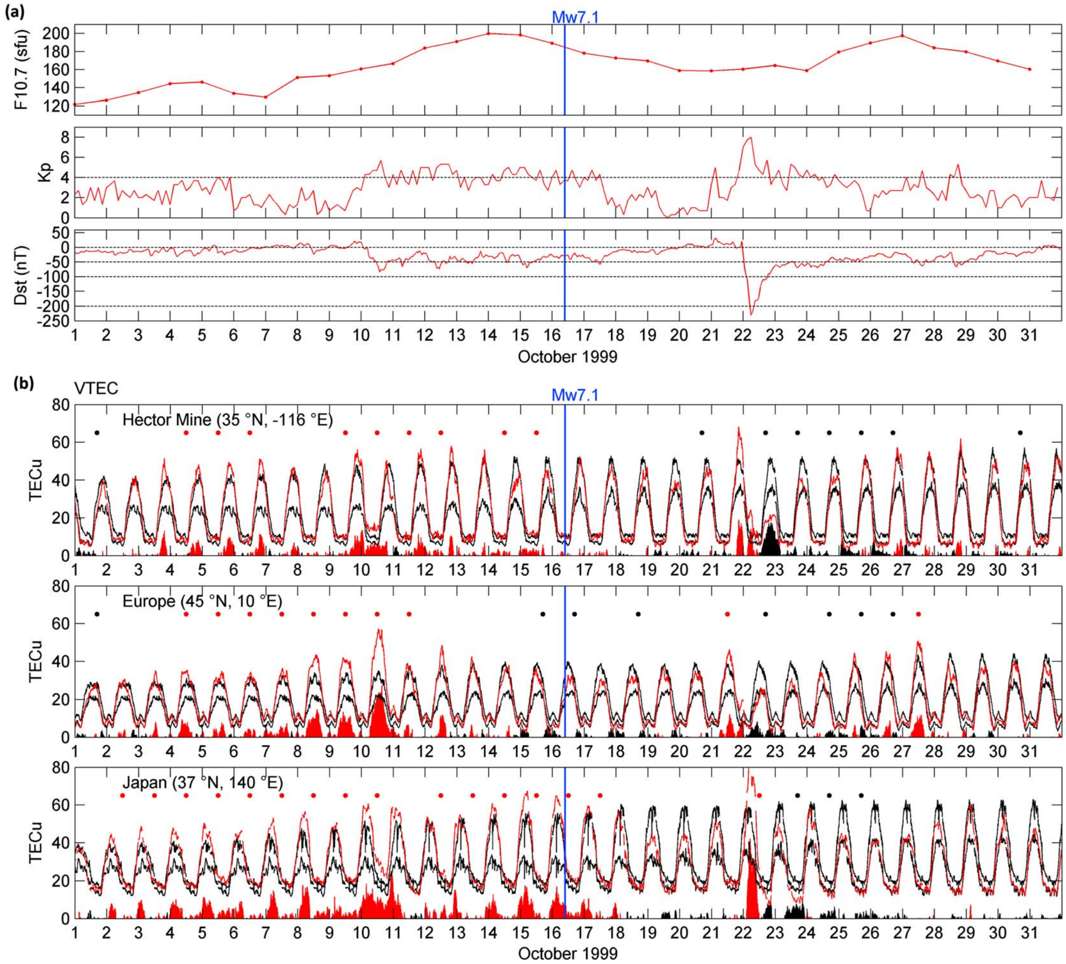

Figure 2. Solar radiation, magnetic condition, and GPS TEC variations during October 1999. (a) The $F_{10.7}$ index and geomagnetic Kp and Dst indices. (b) The GPS TEC over the Hector Mine epicenter, Europe, and Japan areas. The red and two black curves denote observed GPS TEC (O) and associated upper bound (UB) and lower bound (LB), respectively. The LB and UB are constructed by the 1–30 previous days' moving median (M), lower quartile (LQ), and upper quartile (UQ). Here LB = M − 1.5(M − LQ) and UB = M + 1.5(UQ − M). Under the assumption of a normal distribution with mean μ and standard deviation σ for the parameter, the constructed UB and LB are $\mu \pm 1.01\sigma$, respectively. The red/black shaded areas represent the increase/decrease anomalous strength (O-UB/LB-O). The red/black dots denote the anomaly days which the observed GPS TECs exceed the associated UBs/LBs for at least 8 h during 00:00–24:00 UT. The vertical blue line denotes the occurrence of M_w7.1 Hector Mine earthquake. 1 TECU = 10^{16} electrons m^{-2}.

the global ionosphere. Each map consists of 5183 (= 71 × 73) grid points (or lattices). Since the process and area of the earthquake preparation are generally long and huge, the associated SIP duration is most likely long. Therefore, we monitor temporal variations of the GIM TEC and its associated gradient detecting possible SIPs at a given location. When possible SIPs are detected, the distribution and persistence of the TEC anomaly of the 5183 lattices are used to confirm the existence of the detected SIPs. Here we take the Hector Mine earthquake as an example and extract the GIM TEC over the epicenter and compute the associated northward gradient at the epicenter. Figures 4a and 4b reveal that the GIM TEC and its gradient over the epicenter concurrently yield remarkable anomalies on 10 October 1999, which generally agree with Figure 3b that significant decrease anomalies appear during 10–11 October. Therefore, to discriminate global and local effects, we further examine the distributions of increase and decrease anomalies on the 5183 lattices of a sequence of GIMs during 10–11 October 1999. Figures 5a and 5b display the spatial distributions of the increase and decrease anomalies in various persistency periods on 11 October 1999, respectively. It can be seen that when the time goes by, the anomalous lattices vanish gradually and finally remain mainly around the forthcoming Hector Mine epicenter (Text S1 in the supporting information). Figure 5a (5b) shows that the increase (decrease) anomalies of 22 (7) lattices continuously and specifically appear centering at 1500 km southwest (1300 km northeast) from the epicenter during 06:00–24:00 UT (00:00–10:00 UT) on 11 October 1999 which is day 5 before the earthquake. It can be seen that in comparing the earthquake preparation area estimated by *Dobrovolsky et al.* [1979], the increase, especially, and decrease

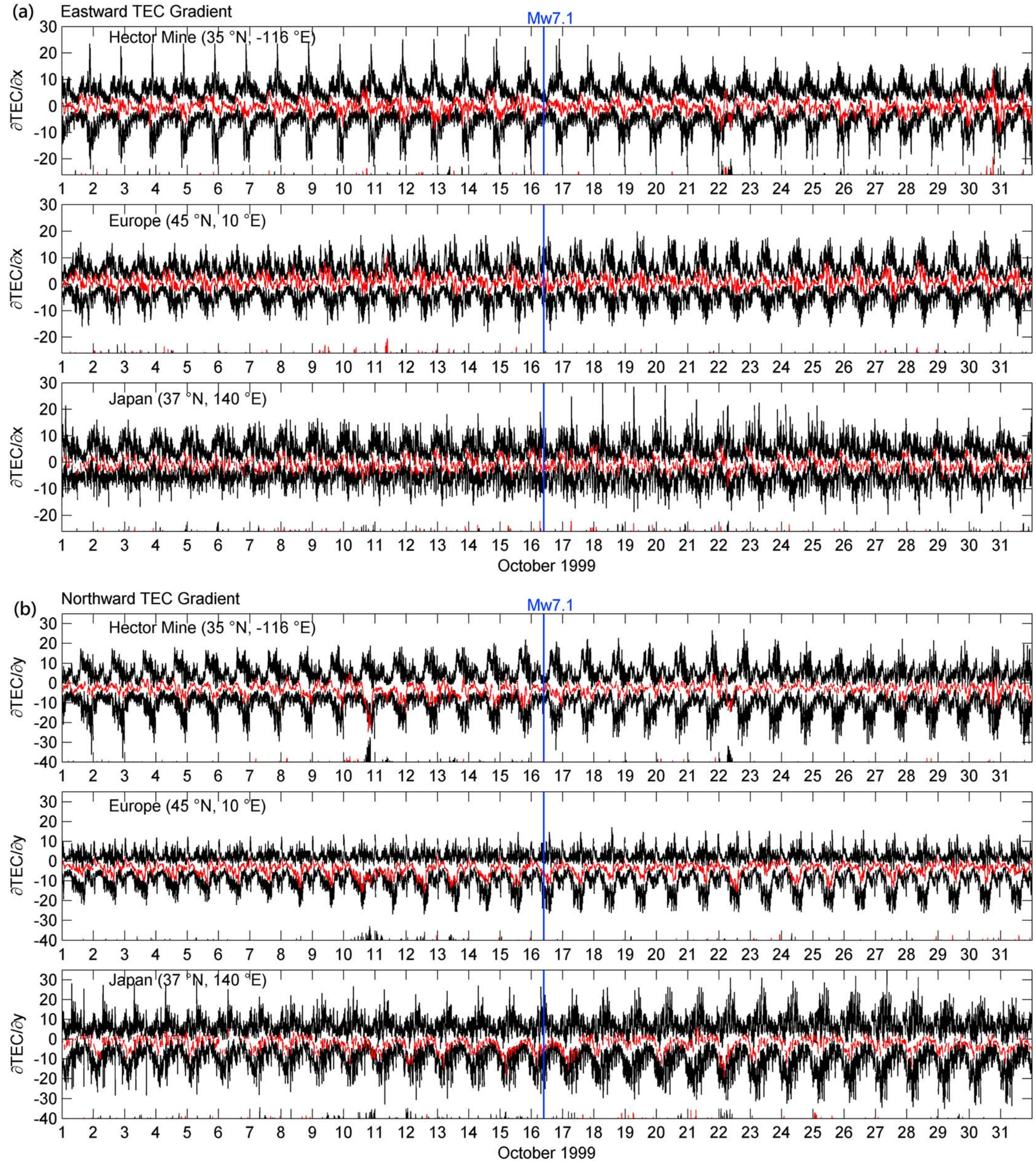

Figure 3. The eastward and northward TEC gradient in three areas during October 1999. The eastward (northward) TEC gradient is defined as the TEC difference between 2° east (north) and 2° west (south) from the epicenter or centers. (a) Eastward and (b) northward TEC gradient over the Hector Mine, Europe, and Japan areas. The red and two black lines denote the observed eastward/northward TEC gradient (O) and the associated upper bound (UB) and lower bound (LB), respectively. The LB and UB are constructed by the 1–30 previous days' moving median (M), lower quartile (LQ), and upper quartile (UQ). Here LB = M – 6 (M – LQ) and UB = M + 6(UQ – M) to detect the very prominent anomaly. Note that the constructed UB and LB are equivalent to $\mu \pm 4.05\sigma$, respectively. The red/black shaded areas represent the increase/decrease anomalous strength (O-UB/LB-O). The unit in *y* axis is TECU in 4°.

anomalies are huge. *Kelley* [2009] shows that the neutral wind, pressure gradient, Lorentz (especially, *E* field) force, and gravity can easily transport the ionospheric plasma. The high mobility of ionospheric plasma response to seismoelectromagnetics generated in the earthquake preparation area results in the extension of the anomalies being so large. In fact, the above increase and decrease anomalies indicate a strong southward gradient which is well in agreement with the decrease anomalies in the northward TEC gradient in the Hector Mine area (Figures 3b and 4b).

3. Discussion and Conclusion

[9] *Pulinets et al*. [2007] examined the regional variability index, the TEC difference between maximum and minimum, of the network of 13 ground-based GPS receivers around the epicenter and reported the growth of the regional variability 5 days before the 1999 M_w7.1 Hector Mine earthquake to be the associated SIP. However, *Thomas et al*. [2012] cross-compared the index of the same GPS network and that of two GPS receivers in high latitudes and concluded that the

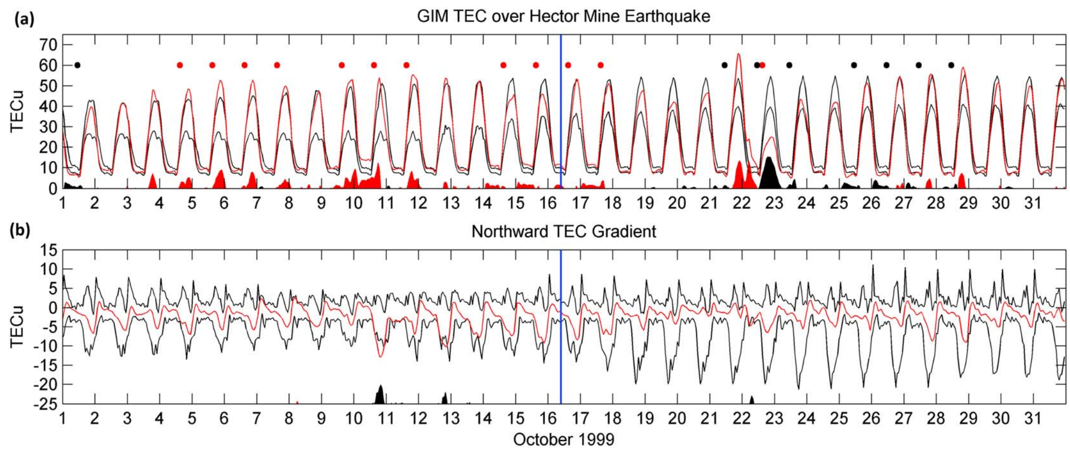

Figure 4. Temporal variations of the TEC and northward gradient in GIM during October 1999. (a) The GPS TEC and (b) northward TEC gradient, which have the same process and criteria in Figures 2b and 3b, respectively, over the Hector Mine epicenter.

anomalous signal identified by *Pulinets et al*. [2007] was just part of normal global-scale TEC variation, which was unrelated to the Hector Mine earthquake. *Thomas et al*. [2012] summarize that the main discrepancies between *Pulinets et al*. [2007] and theirs are the baseline near 8 TECU (total electron content unit; the regional variability index increased during 10–18 October) and the baseline near 12 TECU (the regional variability index increased during 10–16 October), respectively. A detailed study further shows the maximum value in variations of the index of about 80 TECU being obtained by *Thomas et al*. [2012] and 40 TECU by *Pulinets et al*. [2007]. These discrepancies might result from the system bias, cutoff elevation angle, etc., adopted by the two groups being different. Figure 4a illustrates that the TEC extracted from GIM, which agrees with the TEC derived from the Hector Mine network shown in Figure 2b, generally ranges between 5 and 60 TECU. Since the regional variability index is defined as the TEC difference between maximum and minimum observed by a network, in comparing to the GIM TEC range, 80 TECU obtained by *Thomas et al*. [2012] seems to be slightly overestimated. Note that due to satellites orbiting and Earth's rotation, the TEC differences can easily be confounded by nonfixed latitudinal and longitudinal effects. Taking Figure 1 as an example, the regional variability index can significantly be contributed by TEC differences due to the spatial distributions of the GPS satellites and ground-based receiving stations (an image constructed by the subsatellite points of 15° or 1650 km in latitude × 20° or 2200 km in longitude). The GPS orbiting period of 11 h and 56 min results in the TEC image obtained from a receiving network being constantly and daily changed, which makes the regional variability index highly variable and complex. Meanwhile, a smaller cutoff elevation angle could yield a greater image and possibly result in larger changes of the regional variability index. A detailed comparison between *Pulinets et al*. [2007] and *Thomas et al*. [2012] shows that these indices generally yield similar tendencies or trends; however, the data in *Thomas et al*. [2012] are highly spiky. A lower cutoff elevation angle could easily introduce anomalous spikes, and a larger region results in greater tendency values (Text S2). On the other hand, close agreements in the TEC over the Hector Mine and the variability index (the TEC gradient in this study) between *Pulinets et al*. [2007] and our results suggest that the GPS TEC calculation technique used by *Pulinets et al*. [2007] could take care of the effects of GPS subsatellite points changing with time [*Ciraolo*, 2012]. Nevertheless, the regional variability index proposed by *Pulinets et al*. [2007] has an advantage of providing the spatial information. To preserve the advantage and to avoid the possible shortcoming, we propose the TEC gradient around the center of a ground-based GPS network as the other parameter detecting possible SIPs.

[10] Figure 2 shows that many anomalies are observed by the three GPS networks, and the TECs are very sensitive to the solar radiation and storm effects. By contrast, the anomalies in the northward TEC gradients of the three networks prominently and significantly (especially over the Hector Mine region) appear mainly on 10–11 October 1999 (Figure 3). Therefore, the intersection of the TEC and northward gradient can be used to monitor and detect temporal anomaly. Figures 4a and 4b indicate that anomalies appearing on 10–11 October 1999 might be the precursor of a forthcoming earthquake in the Hector Mine area. The increase (decrease) anomalies continuously and specifically appear around the forthcoming epicenter for the duration of 18 (10) h on 11 October 1999 which is day 5 before the earthquake (Figures 5a and 5b). In fact, the spatial distribution of increase and decrease anomalies of GIM TEC shown in Figures 5a and 5b is well in agreement with the decrease anomalies in the northward TEC gradient over the epicenter in Figures 3b and 4b during 10–11 October 1999. This agreement confirms that the TEC data in this study have been correctly processed and indicates that the SIP continuously/specifically appearing over the epicenter during 10–11 October 1999 is associated with the Hector Mine earthquake.

[11] Magnetic storm can simultaneously disturb the global ionosphere [cf. *Liu et al*., 2013b]. For example, *Thomas et al*. [2012] utilized two GPS receivers in high latitudes sensitively detecting the global effect of magnetic storms, while our GPS TEC at the epicenter and the two references also observed significant anomalies during 10–11 October 1999, days 6–5 before the Hector Mine earthquake. Since seismogenerated electromagnetic signals are local effects, the earthquake preparation zone should experience both global

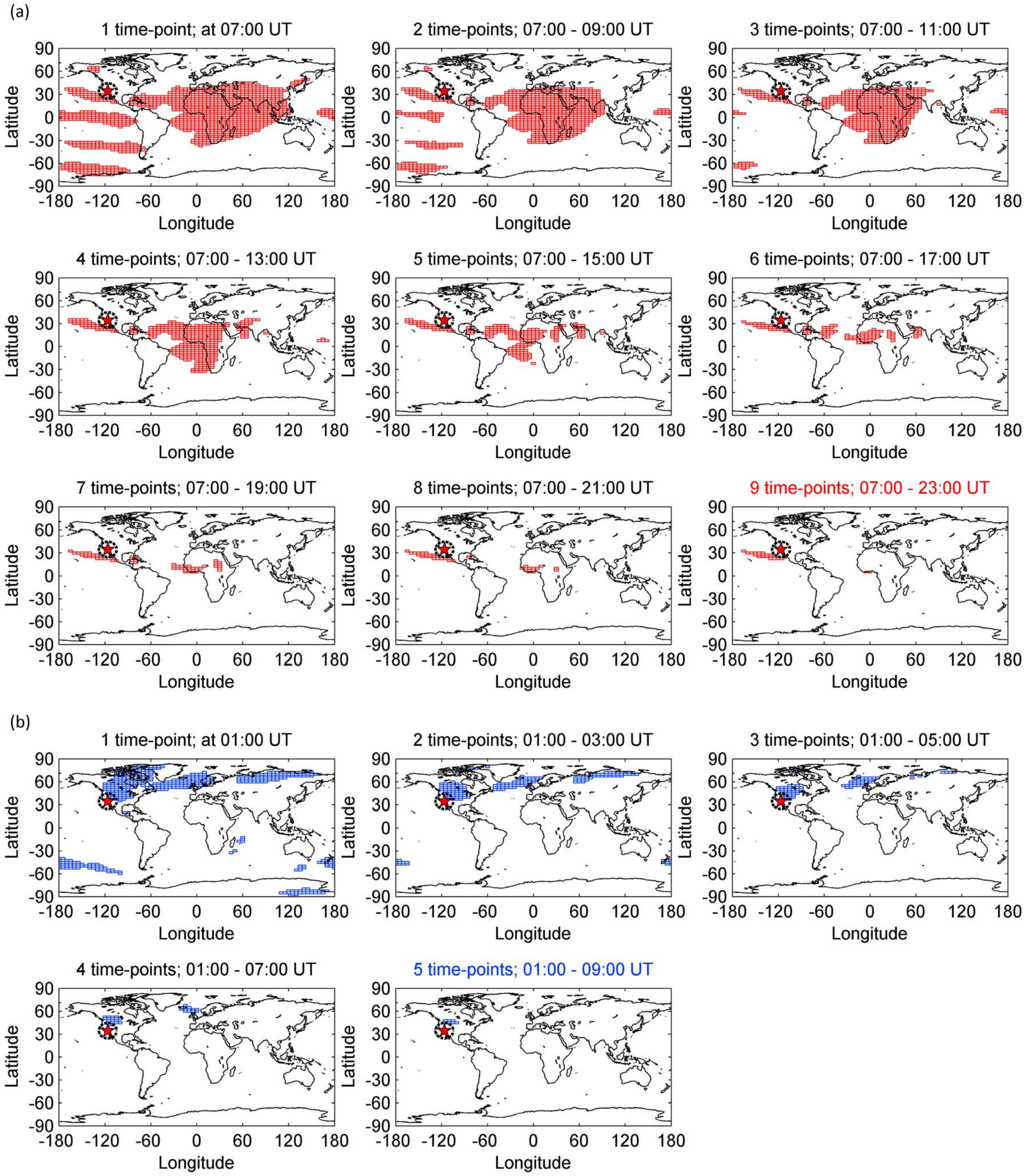

Figure 5. Spatial distributions of the increase and decrease anomalies in various persistency time point periods on 11 October 1999. (a) The increase anomalies from 07:00 to 23:00 UT (nine time points; 08:00–24:00 UT; 18 h) and (b) the decrease anomalies from 01:00 to 09:00 UT (five time points; 00:00–10:00 UT; 10 h). Each time point stands for a 2 h time interval. The red and blue lattices stand for the increase and decrease anomalies in the 10% (=3/30) of largest and least GIM TEC values in comparing with its 1–30 previous days' values observed at the same universal time and lattices, respectively. Each subplot in Figure 5a (or 5b) displays the increase (or decrease) anomalies that continuously appear at certain locations during the specified time point (persistency) period. Note that only the anomalies persistently appearing at a certain location during the specified time point period are denoted in the subplots. For example, at 07.00 UT, 07.00–09.00 UT stand for the persistency of the anomalies during one time point (2 h; 06:00–08:00 UT), two time points (4 h; 06:00–10:00 UT), etc. The last subplots in Figures 5a and 5b display the spatial distributions of increase and decrease anomalies with the longest persistency periods of 18 and 10 h, respectively. The earthquake preparation zone of M_w7.1 Hector Mine earthquake denoted with the dashed circle is computed by using $R = 10^{0.43M}$, where R is the radius of the preparation zone in kilometer and M is the earthquake magnitude [*Dobrovolsky et al.*, 1979].

and local effects. Therefore, limited cross comparisons are very difficult to confirm and/or rule out whether the observed anomalies are related to the earthquake or not. In this paper, we examine the persistency of the increase and decrease anomalies in the 5183 lattices in the GIM TEC to discriminate global and local effects. The increase or decrease anomaly continuously and specifically appearing around the forthcoming epicenter day 5 before the earthquake suggests the GIM global search being informative.

[12] In conclusion, the ionosphere can easily be disturbed by the global effects of solar radiations, solar winds, magnetic storms, etc. The spirit of the regional variability index is useful for detecting SIPs of the GPS TEC. To discriminate global and earthquake-related effects, a spatial analysis on global data sets is required. The temporal and spatial analyses suggest that SIPs of the GPS TEC most likely appear on 10–11 October, days 6–5 before the 16 October 1999 M_w7.1 Hector Mine earthquake. The proposed temporal and spatial analyses should be useful to discriminate anomalies triggered by global effects and local effects, as well as locate possible forthcoming large earthquakes.

[13] **Acknowledgments.** This research work is partially supported by the National Science Council grant NSC102-2628-M-008-001 and the 5Y50B project of National Central University.

[14] Robert Lysak thanks the reviewers for their assistance in evaluating this paper.

References

Afraimovich, E. L., and E. I. Astafyeva (2008), TEC anomalies—Local TEC changes prior to earthquakes or TEC response to solar and geomagnetic activity changes?, *Earth Planets Space*, *60*(9), 961–966.

Chen, Y. I., J. Y. Liu, Y. B. Tsai, and C. S. Chen (2004), Statistical tests for pre-earthquake ionospheric anomaly, *Terr. Atmos. Ocean. Sci.*, *15*, 385–396.

Ciraolo, L. (2012), GNSS derived TEC data calibration, Workshop on Science Applications of GNSS in Developing Countries, Trieste, Italy, 11–27 April 2012.

Dobrovolsky, I. P., S. I. Zubkov, and V. I. Miachkin (1979), Estimation of the size of earthquake preparation zones, *Pure Appl. Geophys.*, *117*, 1025–1044, doi:10.1007/BF00876083.

Hayakawa, M., and O. A. Molchanov (Eds) (2002), *Seismo Electromagnetics: Lithosphere–Atmosphere–Ionosphere Coupling*, p. 477, TERRAPUB, Tokyo.

Jhuang, H. K., Y. Y. Ho, Y. Kakinami, J. Y. Liu, K.-I. Oyama, M. Parrot, K. Hattori, M. Nishihashi, and D. Zhang (2010), Seismo-ionospheric anomalies of the GPS-TEC appear before the 12 May 2008 magnitude 8.0 Wenchuan Earthquake, *Int. J. Remote Sens.*, *31*, 3579–3587, doi:10.1080/01431161003727796.

Kakinami, Y., J. Y. Liu, L. C. Tsai, and K.-I. Oyama (2010), Ionospheric electron content anomalies detected by a FORMOSAT-3/COSMIC empirical model before and after the Wenchuan earthquake, *Int. J. Remote Sens.*, *31*, 3571–3578, doi:10.1080/01431161003727788.

Kelley, M. C. (2009), *The Earth's Ionosphere: Plasma Physics and Electrodynamics*, Elsevier, London, U.K.

Le, H., J. Y. Liu, and L. Liu (2011), A statistical analysis of ionospheric anomalies before 736 M6.0+ earthquakes during 2002–2010, *J. Geophys. Res.*, *116*, A02303, doi:10.1029/2010JA015781.

Le, H., L. Liu, J. Y. Liu, B. Zhao, Y. Chen, and W. Wan (2013), The ionospheric anomalies prior to the M9.0 Tohoku-Oki earthquake, *J. Asian Earth Sci.*, *62*, 476–484, doi:10.1016/j.jseaes.2012.10.034.

Liu, J. Y., Y. I. Chen, S. A. Pulinets, Y. B. Tsai, and Y. J. Chuo (2000), Seismo-ionospheric signatures prior to M>=6.0 Taiwan earthquakes, *Geophys. Res. Lett.*, *27*, 3113–3116, doi:10.1029/2000GL011395.

Liu, J. Y., Y. I. Chen, Y. J. Chuo, and H. F. Tsai (2001), Variations of ionospheric total electron content during the Chi-Chi earthquake, *Geophys. Res. Lett.*, *28*, 1383–1386, doi:10.1029/2000GL012511.

Liu, J. Y., Y. J. Chuo, S. J. Shan, Y. B. Tsai, Y. I. Chen, S. A. Pulinets, and S. B. Yu (2004), Pre-earthquake ionospheric anomalies registered by continuous GPS TEC measurements, *Ann. Geophys.*, *22*, 1585–1593, doi:10.5194/angeo-22-1585-2004.

Liu, J. Y., Y. I. Chen, Y. J. Chuo, and C. S. Chen (2006), A statistical investigation of pre-earthquake ionospheric anomaly, *J. Geophys. Res.*, *111*, A05304, doi:10.1029/2005JA011333.

Liu, J. Y., et al. (2009), Seismo-ionospheric GPS total electron content anomalies observed before the 12 May 2008 M_w7.9 Wenchuan earthquake, *J. Geophys. Res.*, *114*, A04320, doi:10.1029/2008JA013698.

Liu, J. Y., Y. I. Chen, C. H. Chen, and K. Hattori (2010), Temporal and spatial anomalies in the ionospheric GPS total electron content observed before the 26 December 2004 M9.3 Sumatra-Andaman Earthquake, *J. Geophys. Res.*, *115*, A09312, doi:10.1029/2010JA015313.

Liu, J. Y., H. Le, Y. I. Chen, C. H. Chen, L. Liu, W. Wan, Y. Z. Su, Y. Y. Sun, C. Lin, and M. Q. Chen (2011), Observations and simulations of seismo-ionospheric GPS total electron content anomalies before the 12 January 2010 M7 Haiti earthquake, *J. Geophys. Res.*, *116*, A04302, doi:10.1029/2010JA015704.

Liu, J. Y., K. Wang, C. H. Chen, W. H. Yang, Y. H. Yen, Y. I. Chen, K. Hatorri, H. T. Su, R. R. Hsu, and C. H. Chang (2013a), A statistical study on ELF-whistlers/emissions and M≥5.0 earthquakes in Taiwan, *J. Geophys. Res. Space Physics*, *118*, 3760–3768, doi:10.1002/jgra.50356.

Liu, J. Y., W. H. Yang, C. H. Lin, Y. I. Chen, *and* I. T. Lee (2013b), A statistical study on the characteristics of ionospheric storms in the equatorial ionization anomaly region: GPS-TEC observed over Taiwan, *J. Geophys. Res. Space Physics*, *118*, 3856–3865, *doi*:10.1002/jgra.50366.

Pulinets, S. A., and K. A. Boyarchuk (2004), *Ionospheric Precursors of Earthquakes*, p. 315, Springer, Berlin, Germany.

Pulinets, S. A., A. N. Kotsarenko, L. Ciraolo, and I. A. Pulinets (2007), Special case of ionospheric day-to-day variability associated with earthquake preparation, *Adv. Space Res.*, *39*, 970–977, doi:10.1016/j.asr.2006.04.032.

Thomas, J. N., J. J. Love, A. Komjathy, O. P. Verkhoglyadova, M. Butala, and N. Rivera (2012), On the reported ionospheric precursor of the 1999 Hector Mine, California earthquake, *Geophys. Res. Lett.*, *39*, L06302, doi:10.1029/2012GL051022.

Zhao, B., M. Wang, T. Yu, W. Wan, J. Lei, L. Liu, and B. Ning (2008), Is an unusual large enhancement of ionospheric electron density linked with the 2008 great Wenchuan earthquake?, *J. Geophys. Res.*, *113*, A11304, doi:10.1029/2008JA013613.